

Dynamics of Two Granules

Alexandre Rosas, J. Buceta, and Katja Lindenberg
*Department of Chemistry and Biochemistry, and Institute for Nonlinear
 Science University of California San Diego La Jolla, CA 92093-0340*
 (Dated: May 26, 2020)

We study the dynamics of two particles that interact only when in contact. In this sense, although not in every particular, the interactions mimic those in granular materials. The detailed solution of the dynamics allows an analysis of the backscattering behavior of the first particle and of the energy dissipation in the system as a function of various parameters.

PACS numbers: 45.70.-n, 05.45.-a, 45.05.+x

I. INTRODUCTION

Signal propagation in granular materials is a long-standing subject of interest [1, 2, 3, 4, 5], and has recently attracted considerable attention in a number of novel contexts. One is the observation that the attenuation characteristics of signals (impacts) in such materials might make them good candidates for shock absorption [6]. Another is the use of the backscattered signal for the nondestructive identification of buried objects [5, 7, 8, 9, 10].

Interactions in granular materials are notoriously complex, but a number of relatively simple models have been implemented in the context of signal propagation, models that it is hoped capture the principal ingredients of the true interactions at least in some regimes. A model potential used for a monodisperse chain of particles that repel upon overlap according to the Hertz law is given by [11]

$$\begin{aligned} V(\delta_{i,i+1}) &= a\delta_{i,i+1}^n, & \delta \leq 0, \\ V(\delta_{i,i+1}) &= 0, & \delta > 0. \end{aligned} \quad (1)$$

Here

$$\delta_{i,i+1} \equiv 2R - [(z_{i+1} + x_{i+1}) - (z_i + x_i)], \quad (2)$$

$$a = \frac{2}{5D(Y,\sigma)} \left(\frac{R}{2}\right)^{1/2}, \quad D(Y,\sigma) = \frac{3}{2} \left(\frac{1-\sigma^2}{Y}\right), \quad (3)$$

Y and σ denote Young's modulus and Poisson's ratio, z_i denotes the initial equilibrium position of grain i in the chain, and x_i is the displacement of grain i from this equilibrium position. The geometric parameter R is the radius if the particles are elastic spheres. More generally, R is determined by the principal radii of curvature of the surfaces at the point of contact [12]. The exponent n is 5/2 for spheres, it is 2 for cylinders, and in general depends on geometry.

Two features of the potential are decisive for the resulting propagation properties of the chain: one is the exponent n , and the other is the absence of an attractive portion in the potential. It is in this latter respect that the granular chain differs profoundly from the many models of nonlinearly interacting oscillators (such as the Fermi-Pasta-Ulam chain) extensively studied in recent years [13, 14].

Two decades ago Nesterenko [3] showed that under appropriate assumptions, among them the slow spatial variation of the displacements x_i , the equations of motion for the granular particles could be approximated by a continuous nonlinear partial differential equation that admits a soliton solution for a propagating perturbation in the chain. More recently it was shown that strictly speaking these solutions are solitary waves rather than solitons [15, 16]. It is also understood that a potential exponent $n > 2$ is required to accommodate solitary waves, i.e. that a "hard nonlinearity" is required [6]. Nesterenko coined the words "sonic vacuum" to stress the importance of the absence of "harmonic terms" ($n = 2$) in this analysis because such terms (and only such terms) are associated with ordinary sound propagation. Indeed, as $n \rightarrow 2$ the width of the solitary wave diverges. More recently, numerical simulations of *discrete* chains have provided a great deal of additional information about the important role of discreteness as well as nonlinearity in the signal propagation properties.

Thus, while the continuum solitary wave solutions provide enormously helpful analytic insights, the importance of discreteness in the propagation properties of such chains should not be underestimated. Neither should the fact that even with a "harmonic" exponent $n = 2$, the chain is decidedly different from a harmonic system *because there is no*

attractive restoring force. The resulting nonanalyticity of the potential leads to profoundly different properties than those observed in an ordinary harmonic chain. Indeed, although solitary waves are no longer exact solutions (and there is no longer a perfect sonic vacuum), there are extremely long lived quasi-solitary waves that broaden slowly (whereas a harmonic chain would exhibit rapid dispersion of energy) [14].

We offer the above observations in support of the usefulness of a study of a chain with only repulsive forces even with the choice $n = 2$. A number of helpful insights can be achieved from such a study if one is able to obtain analytic results, and this is at all possible only with $n = 2$. In this paper we carry out such an analysis for the simplest (and yet extremely interesting) such system, namely, one consisting of only two masses. Surprisingly, this simple scenario seems not to have been analyzed in detail in the literature, although the dynamics of pairwise collisions is an important input (and phenomenological assumptions are made about it) in the study of longer chains [5]. A two-mass system, being explicitly integrable, can yield valuable information. In view of some of the current applications of energy propagation in granular materials, we are particularly interested in *backscattering* and *energy dissipation* in the presence of friction, and on the effects of frictional disorder on these quantities. The results of our analysis promise to provide helpful phenomenological input into the propagation of excitation pulses in longer chains as long as the pulses remain narrow. For example, recent experiments on impulse dispersion in tapered chains indicate the significant role of friction in the propagation and dispersion process [17]. We find that a two-mass system leads to some unanticipated nonmonotonic (albeit, in hindsight understandable) behaviors as one varies system parameters. To support the relevance of our results to the spherical granular problem, we also present some numerical results for the Hertz potential with $n = 5/2$ and show the similarity in the behavior of this system and that of the $n = 2$ case.

We consider two finite-sized particles (“granules”) of equal mass m . The specific value of the mass does not matter since it can be scaled out by redefining variables; the only important point is that the masses are equal. When the granules “do not touch”, each moves independently of the other (i.e., their potential of interaction is zero beyond a certain distance between their centers). When they *do* “push one into the other”, there is a repulsive linear force between their centers with force constant k ; the force vanishes once the particles separate again. One or both of the granules are subject to friction, which may be kinetic (i.e. constant, see Sec. II) or hydrodynamic (i.e. proportional to velocity, see Sec. III). In order to initiate energy transfer between the granules, one can, for example, introduce some precompression in the system, or one can impart one of the granules an initial velocity toward the other. We do the latter: initially the granules are assumed to be just touching, the first granule has initial velocity v_0 toward the second, and the second is at rest. We are interested in the velocity of the two granules and the total energy in the system *immediately after the collision*. Note that in the absence of friction the collision is elastic so that the energy and momentum are conserved. In this case the first granule simply ends up at rest and the second with velocity v_0 , i.e., there is no backscattering. Of course there is backscattering, even in the absence of friction, in a longer chain.

Even these simple systems present a broad range of outcomes, some more interesting than others, and not all of which will be covered in detail. For example, one or the other or both granules may stop moving altogether before the collision is over. However, we are particularly interested in situations where the second granule is still moving forward after the collision (propagation) and the first granule is moving backward (backscattering). Our analysis will focus on these outcomes and the conditions that lead to them.

In Sec. II we present and solve the two-particle model with kinetic friction. Section III presents a similar calculation for the model with hydrodynamic friction. A summary of results, and a brief outlook of future work, are gathered in Sec. IV.

II. TWO PARTICLES WITH KINETIC FRICTION

In this section we examine granule collision when one or both of the granules are subject to kinetic friction with friction coefficient μ . Kinetic friction arises from contact forces when a solid body moves along a solid surface, and depends on the velocity only in that its direction is always opposed to the velocity. Two cases are presented analytically (at least in part). They turn out to exhibit rather different behaviors, which we anticipate here as a point of reference. In one, only the second granule is subject to friction. We find that for a certain range of friction coefficient values there is both propagation and backscattering, that the velocities of the forward moving second granule and the backward moving first granule are monotonic functions of the friction, but that the total energy dissipation during the collision is nonmonotonic. In the second model only the first granule is subject to friction. Here we again find a range of values of the friction coefficient for which there is both propagation and backscattering. Now, however, the granule velocities are nonmonotonic functions of the friction while the energy loss is a monotonic function. Results for the more general case of both granules subject to (possibly different) friction are presented numerically. In this way we cover the entire range of “frictional disorder”, as might occur if the granules are made of different materials. While most of our discussion revolves around the case $n = 2$, some results for $n = 5/2$ are presented. Also, as a backdrop we keep in mind the most extreme case of a hard interaction, a hard sphere ($n \rightarrow \infty$). The interaction is instantaneous

in this case and leads to elastic collisions in which energy and momentum are conserved. The first granule stops and the second granule moves forward. This comment emphasizes the observation that only collisions of finite duration can lead to a combination of backscattering and propagation in two granules.

We rescale variables (see Appendix A) so that we can set the coefficient $a \equiv 1$ in Eq. (1) regardless of the value of n . This rescaling allows presentation of results in terms of a single parameter, the scaled friction.

A. Frictionless First Granule

Consider first the case of a frictionless first granule. The movement of the second granule will then only start if the elastic compression exceeds the frictional force, $x_1^{n-1} > \eta$, and so at first only the first granule moves and its motion is governed by the equation of motion

$$\ddot{x}_1(t) = -[x_1(t)]^{n-1}. \quad (4)$$

The initial condition for this problem is $x_1(0) = 0$ and $\dot{x}_1(0) = 1$. The solution for $n = 2$ is easily found to be

$$x_1(t) = \sin(t), \quad (5)$$

and is valid until the time t_0 at which $x_1(t_0) = \eta$, that is, until $t_0 = \arcsin(\eta)$.

At time t_0 the second granule starts moving as well, and the system is now governed by the two coupled equations of motion

$$\ddot{x}_1(t') = -[x_1(t') - x_2(t')] \quad (6a)$$

$$\ddot{x}_2(t') = -\eta - [x_2(t') - x_1(t')] \quad (6b)$$

with the initial conditions: $x_1(t' = 0) = \eta$, $\dot{x}_1(t' = 0) = \sqrt{1 - \eta^2}$, and $x_2(t' = 0) = \dot{x}_2(t' = 0) = 0$. Here we have defined $t' = t - t_0$. The solution is found to be:

$$x_1(t') = \frac{1}{4} \left[-\eta(-3 + t'^2) + 2(1 - \eta^2)^{1/2}t' + \eta \cos(\sqrt{2}t') + \sqrt{2}(1 - \eta^2)^{1/2} \sin(\sqrt{2}t') \right] \quad (7a)$$

$$x_2(t') = -\frac{1}{4} \left[\eta(-1 + t'^2) - 2(1 - \eta^2)^{1/2}t' + \eta \cos(\sqrt{2}t') + \sqrt{2}(1 - \eta^2)^{1/2} \sin(\sqrt{2}t') \right]. \quad (7b)$$

If η is too large, the second granule will stop before the two granules lose contact. For sufficiently small η this does not happen and the above solutions then remain valid until contact is lost. The time $t' = t_1$ when this occurs is the time at which $\Delta x(t_1) = x_1(t_1) - x_2(t_1)$ vanishes, that is, when $t_1 = \pi/\sqrt{2}$. The velocities of the granules at the moment of separation $t = t_0 + t_1$ are

$$v_1^{(s)} = -\frac{\eta\pi}{2\sqrt{2}} \quad (8a)$$

$$v_2^{(s)} = \left((1 - \eta^2)^{1/2} - \frac{\eta\pi}{2\sqrt{2}} \right). \quad (8b)$$

The values of η for which this description is valid are those for which $v_2^{(s)} > 0$, that is, for $0 < \eta < (1 + \pi^2/8)^{-1/2} = 0.669\dots$. Beyond time $t = t_0 + t_1$ each granule continues on its course, the first forever and the second until friction brings it to rest. Backscattering and propagation thus occur when $\eta < 0.669\dots$. As a function of η in this range, the magnitude of the backward velocity increases monotonically while that of the forward velocity decreases monotonically. The backscattering is shown in Fig. 1, which we exhibit in order to stress the similarity in the behavior of the $n = 2$ potential and that of the Hertz potential for spheres. As n increases the range of η for which both $v_1^{(s)}$ and $v_2^{(s)}$ are nonzero shrinks, until it shrinks away completely for a hard sphere potential.

Perhaps the most dramatic outcome of this calculation is the fact that *the friction on the second granule causes the first granule to move backward* (recall that if both granules are frictionless the first one simply stops). In other words, the friction on the second granule is responsible for backscattering. This behavior, strange at first glance, occurs because the first granule “stops too soon”, that is, it stops before the spring has had time to decompress completely. Indeed, if the friction on the second granule is so strong that it does not move at all, the first will move backward with velocity $v_1 = -1$. Our model lies between the limiting cases of zero and very large η ($-1 \leq v_1^{(s)} \leq 0$).

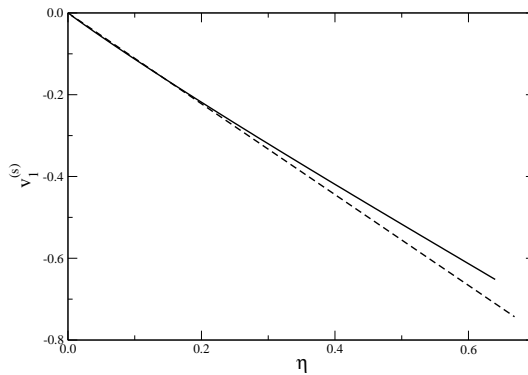


FIG. 1: Velocity of the first (frictionless) granule at the end of the collision as a function of friction. Solid curve: $n = 2.5$ (Hertz potential for spheres). Dashed curve: $n = 2$.

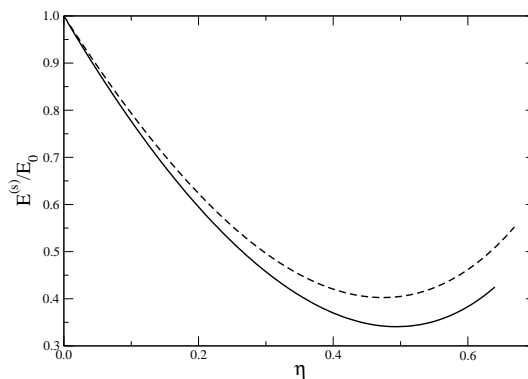


FIG. 2: Ratio of the total energy at the moment of separation to the initial energy as a function of friction. Solid curve: $n = 2.5$ (Hertz potential for spheres). Dashed curve: $n = 2$.

In Fig. 2 we show the ratio of the total kinetic energy of the system at the end of the collision to the initial energy,

$$\frac{E^{(s)}}{E_0} = 1 - \frac{\eta(1-\eta^2)^{1/2}\pi}{\sqrt{2}} + \left(\frac{\pi^2}{4} - 1\right)\eta^2. \quad (9)$$

In the rescaled variables, $E_0 = 1/2$. Curiously, there is a region where this ratio *increases* with increasing friction coefficient. The reason for this behavior is that when friction increases beyond a certain point (beyond the minimum in the curve), relatively more energy is transferred to the first granule (as opposed to being simply dissipated) by the end of the collision. Again we also show the numerical results obtained for the Hertz potential with $n = 5/2$ (solid curve) and comment on the similarity with the $n = 2$ curve.

B. Frictionless Second Granule

Next we consider the case of a frictionless second granule. The first granule now moves forward, eventually stops, and *perhaps* moves backward, while the second granule moves forward.

As before, the granules are initially just touching, the first granule having an initial velocity $v_0 \equiv 1$. While the first granule is moving forward the system is governed by the equations

$$\ddot{x}_1(t) = -\eta - [x_1(t) - x_2(t)] \quad (10a)$$

$$\ddot{x}_2(t) = -[x_2(t) - x_1(t)]. \quad (10b)$$

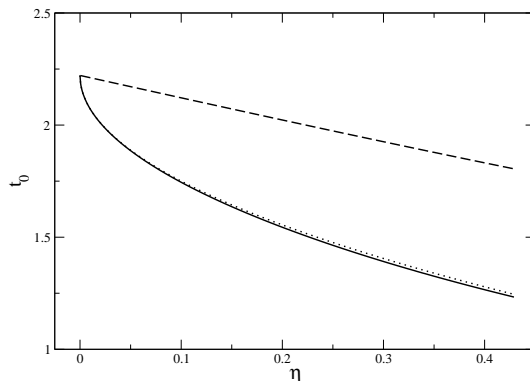


FIG. 3: Comparison of the small- η analytical solution (dotted) and the numerical solution (solid) of the stopping condition $v_1(t_0) = 0$. The dashed line is the time it would take the granules to separate if the solutions (11a) and (11b) remained valid until then. The fact that it lies above the other curves indicates that the first granule stops before the collision is over.

Explicit integration yields

$$x_1(t) = \frac{1}{4} \left[-\eta + 2t - \eta t^2 + \eta \cos(\sqrt{2}t) + \sqrt{2} \sin(\sqrt{2}t) \right] \quad (11a)$$

$$x_2(t) = \frac{1}{4} \left[\eta + 2t - \eta t^2 - \eta \cos(\sqrt{2}t) - \sqrt{2} \sin(\sqrt{2}t) \right]. \quad (11b)$$

These equations hold as long as the velocity $v_1(t) = \dot{x}_1(t) > 0$. This velocity is given by

$$v_1(t) = \frac{1}{4} \left[2 - 2\eta t + 2 \cos(\sqrt{2}t) - \sqrt{2}\eta \sin(\sqrt{2}t) \right]. \quad (12)$$

The time t_0 at which $v_1(t_0) = 0$ cannot be found explicitly in general, but the problem may still be treated analytically for small or for large η , or numerically for arbitrary η .

If $\eta \ll 1$, we can expand $v_1(t)$ around $t = \pi/\sqrt{2}$ (the solution for $\eta = 0$). We find that

$$t_0 = \frac{\pi}{\sqrt{2}} - \left(\frac{\pi\eta}{\sqrt{2}} \right)^{1/2} + \mathcal{O}(\eta^{3/2}). \quad (13)$$

In Fig. 3 we compare this analytical approximation with the numerical solution. The small- η approximation is clearly very good for a rather large range of η . Therefore, we proceed using this approximation. In the figure we also show the time that it would take the collision to be over if the solutions (11a) and (11b) would remain valid, i.e., the solution t'_0 of the equation $x_1(t'_0) = x_2(t'_0)$. This time, shown as a dashed line, is always above the time at which the first granule stops, indicating that the first granule *necessarily* stops before the collision is over. This persists even for large η : as $\eta \rightarrow \infty$ the stopping time of the first granule goes to zero as $1/\eta$, while the time for the collision to be over if the above solutions would remain valid goes to zero as $2/\eta$.

When the first granule stops, the equations of motion are no longer Eqs. (10a) and (10b). The initial conditions for the new set of equations are the velocities and positions found above at time $t = t_0$. Within the small- η approximation we use

$$x_1(t_0) = \frac{1}{8} \left[2\sqrt{2}\pi - (\pi^2 + 4)\eta \right] \quad (14a)$$

$$x_2(t_0) = \frac{1}{8} \left[2\sqrt{2}\pi - 4(2^{3/4})\sqrt{\pi\eta} - (\pi^2 - 4)\eta \right] \quad (14b)$$

$$v_1(t_0) = 0 \quad (14c)$$

$$v_2(t_0) = \frac{1}{2} \left[2 - \sqrt{2}\pi\eta \right] \quad (14d)$$

as the initial conditions.

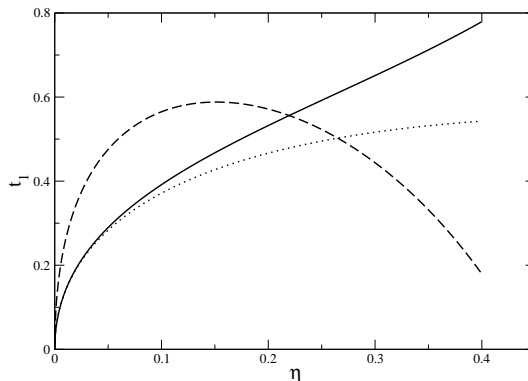


FIG. 4: Comparison of time required for the two granules to separate calculated numerically (solid) and analytically for small η (dotted). The time required for the first granule to stop according to the equations of motion (16a) and (16b) is shown as a dashed curve. Therefore, if $\eta \lesssim 0.22$ the first granule is still moving backwards at the end of the collision.

The equations of motion at this point depend on whether the first granule simply remains stationary or starts moving backward. The latter occurs if the elastic force is greater than the friction, that is, if

$$[x_1(t_0) - x_2(t_0)] = \frac{1}{2} \left[-\eta - \eta \cos(2^{1/4} \sqrt{\eta\pi}) + \sqrt{2} \sin(2^{1/4} \sqrt{\eta\pi}) \right] > \eta. \quad (15)$$

Therefore, for η smaller than a critical value ($\eta = 0.439\dots$) the first granule will start moving backward, and we confine our analysis to this case. The equations of motion then are (note that since the first granule is moving backward, the friction is also reversed):

$$\ddot{x}_1(t') = \eta - [x_1(t') - x_2(t')] \quad (16a)$$

$$\ddot{x}_2(t') = -[x_2(t') - x_1(t')] \quad (16b)$$

where $t' = t - t_0$. The initial conditions are those given in Eqs. (14a)-(14d).

The solutions of this set as a series in η can easily be exhibited explicitly but are not very instructive. Two cases must be distinguished: 1) The first granule is still moving backward when the collision ends; and 2) The first granule stops before the collision ends, at which point the equation of motion (16a) no longer holds. In either case, from the series solutions one can calculate the time $t' = t_1$ at which the collision ends as the solution of the equation $x_1(t') = x_2(t')$. If we assume that the first granule is still moving we find

$$t_1 = \left(\frac{\pi\eta}{\sqrt{2}} \right)^{1/2} - \eta + \mathcal{O}(\eta^{3/2}). \quad (17)$$

This solution is shown as the dotted curve in Fig. 4, as is the numerically obtained exact solution (solid line). The approximation (17) begins to seriously deviate from the exact solution at around $\eta \sim 0.1$. The dashed curve indicates the time at which the first granule stops before the end of the collision if Eq. (16a) remains valid until it does. This analysis is therefore appropriate and leads to backscattering (and propagation) if $\eta \lesssim 0.22$.

In Fig. 5 we see that as η increases the final backward velocity of the first granule is nonmonotonic, that it, increases from zero to approximately 3% of the initial velocity, and then decreases again. In this model, we thus observe that there is backscattering for small η . For $\eta = 0$ and for η greater than a certain value ($\gtrsim 0.22$), the first granule is at rest when the collision ends and there is no backscattering. Therefore, the backscattering in this model happens because the *first* granule (as opposed to the second granule in the previous example) “stops too soon” (i.e. before the collision is over), but not “too late” (i.e. when the compression is still strong enough to overcome friction). The required balance leads to the nonmonotonic behavior seen in Fig. 5. Even though the backscattering is small (e.g. compared to that in the first model), it is conceptually striking. However, the total energy of the system at the end of the collision is a monotonically decreasing function of η , in contrast to the behavior in the previous case shown in Fig. 2.

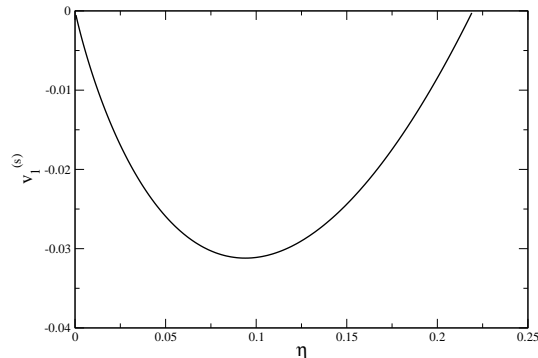


FIG. 5: Final velocity of the first granule.

C. Granules with Arbitrary Friction

While the results presented above deal with the extremes of frictional disorder, it is helpful to present a broad brush of graphical results for arbitrary combinations of η_1 and η_2 , the friction parameters for the two granules. This is also an opportunity for re-assertion that these broad brush results are essentially the same for the $n = 2$ and the $n = 5/2$ Hertz potentials for two granules. Since the graphical results are necessarily numerical, we present them for the $n = 5/2$ potential. They are qualitatively indistinguishable from those for $n = 2$.

In Fig. 6 we show in gray scale the magnitudes of $v_1^{(s)}$ (first panel), $v_2^{(s)}$ (second panel) and energy ratio $E^{(s)}/E_0$ at the end of the collision in the (η_1, η_2) regime where there is simultaneous backscattering and propagation. Darker shading represents a higher speed (first and second panels) and a higher energy (third panel). Figure 1 is associated with an upward trajectory in the first panel at $\eta_1 = 0$. The monotonically increasing backscattering seen in Fig. 1 corresponds to the upward darkening. Figure 2 is associated with the same upward trajectory, now in the rightmost panel. The nonmonotonicity is seen in the lightening followed by darkening. The nonmonotonicity of Fig. 5 is associated with the shading in the first panel associated with the horizontal trajectory along $\eta_2 = 0$, captured in the curvature of the iso-velocity lines. The monotonicity of $v_2^{(s)}$ discussed in the $(\eta_1, 0)$ and $(0, \eta_2)$ cases is evident in the middle panel.

This rather complex behavior arises from the interplay of energy dissipation and energy transfer during a collision. Thus, for example, increasing friction on the first granule causes it to stop sooner. If it stops too soon (“high η_1 ”), the spring is not sufficiently compressed to overcome friction and it may happen that the whole process simply stops then and either one or the other or both granules do not move. On the other hand, if it stops too late (“low η_1 ”) then the energy transfer to the second granule may cause it to move forward, but there may not be sufficient energy to cause backscattering. Or backscattering may occur but not forward motion. Between these situations (“intermediate η_1 ”), both granules may be in motion at the end of the collision.

III. TWO PARTICLES WITH HYDRODYNAMIC FRICTION

When dissipation is of hydrodynamic origin, the dissipative force is proportional to the particle velocity, $-\gamma\dot{x}$. Hydrodynamic friction arises from the motion of a body against a lubricated surface or in a liquid or gaseous medium. We find that the cases of equal and slightly unequal friction coefficients can be solved analytically and cover essentially the whole spectrum of possible behaviors.

The scaled equations of motion (see Appendix A) for the potential with $n = 2$ are

$$\ddot{x}_1(t) = -\gamma_1\dot{x}_1 - [x_1(t) - x_2(t)] \quad (18a)$$

$$\ddot{x}_2(t) = -\gamma_2\dot{x}_2 - [x_2(t) - x_1(t)] \quad (18b)$$

Even though these equations can be integrated exactly, the time required for the two granules to separate can, in general, only be calculated numerically. Here we consider the case $\gamma_1 \approx \gamma_2$, for which we can find an approximate analytic expression for this time. Thus, we set $\gamma_i = \gamma(1 + \delta_i)$ with $\delta_1 = -\delta_2 \equiv \delta$ and solve the problem for small $|\delta|$.

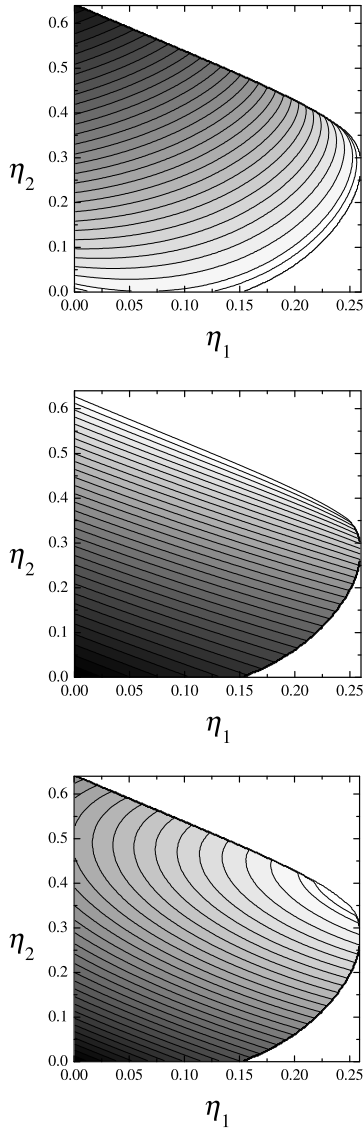


FIG. 6: Backscattering velocity $-v_1^{(s)}$ (first panel), forward velocity $v_2^{(s)}$ (second panel), and energy ratio $E^{(s)}/E_0$ (third panel) at the end of a collision for the Hertz potential for spheres. In the first two the gray scale shows darker coloring for higher speeds. In the third panel darker coloring indicates higher energy. The curves in the first two panels are iso-velocity lines, and in the third panel iso-energy lines.

Defining $x_{\pm} = x_1 \pm x_2$, we can obtain from Eqs. (18) the associated Laplace transforms $X_{\pm}(s)$:

$$\delta\gamma s X_-(s) + (\gamma s + s^2) X_+(s) = 1 \quad (19a)$$

$$(2 + \gamma s + s^2) X_-(s) + \delta\gamma s X_+(s) = 1. \quad (19b)$$

The solution of these equations to first order in δ is

$$X_+(s) = \frac{1}{s(\gamma + s)} - \frac{\delta\gamma}{s(\gamma + s)[2 + s(\gamma + s)]} \quad (20a)$$

$$X_-(s) = \frac{1}{2 + s(\gamma + s)} - \frac{\delta\gamma}{(\gamma + s)[2 + s(\gamma + s)]}. \quad (20b)$$

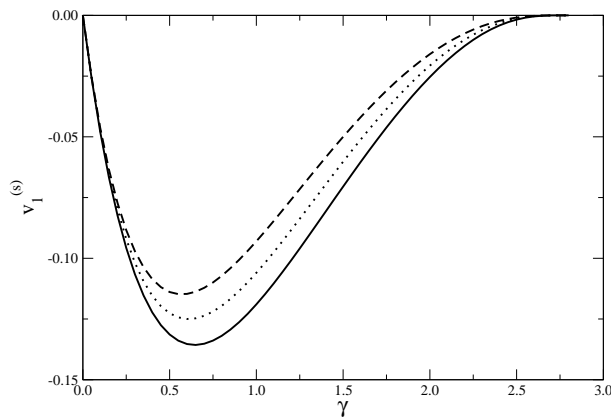


FIG. 7: Final velocity of the first granule when $\gamma_1 > \gamma_2$, $\delta = 0.1$ (dashed), $\gamma_1 = \gamma_2$, $\delta = 0$ (dotted), and $\gamma_1 < \gamma_2$, $\delta = -0.1$ (solid).

The time functions $x_{\pm}(t)$ are the inverse Laplace transforms of $X_{\pm}(s)$. Furthermore, the time t_0 at which the granules separate can be calculated by solving the equation $x_{-}(t = t_0) = 0$. To zeroth order in δ (that is, for $\delta = 0$), we have

$$x_{-}(t_0) = e^{-\gamma t_0/2} \frac{\sin(\omega t)}{\omega} = 0, \quad (21)$$

where $\omega = \sqrt{8 - \gamma^2}/2$. If $\gamma^2 \geq 8$ the collision never ends. If $\gamma^2 < 8$ then it ends at time $t_0 = \pi/\omega$. To calculate the separation time to first order in δ , we write $t_1 = t_0 + \epsilon/\omega$, expand $x_{-}(t_1) = 0$ to first order in ϵ , and solve the resulting equation for ϵ , to obtain

$$\epsilon = -\frac{\delta\gamma\omega}{2} \left(1 + e^{-\gamma\pi/2\omega}\right). \quad (22)$$

The final velocities of the granules at the end of the collision to first order in δ are:

$$v_1^{(s)} = \frac{1}{2} \left(1 - e^{\gamma\pi/2\omega}\right) e^{-\gamma\pi/\omega} + \frac{\delta\gamma^2}{4} \left(1 + 2e^{\gamma\pi/2\omega} + e^{\gamma\pi/\omega}\right) e^{-3\gamma\pi/2\omega} \quad (23a)$$

$$v_2^{(s)} = \frac{1}{2} \left(1 + e^{\gamma\pi/2\omega}\right) e^{-\gamma\pi/\omega} + \frac{\delta\gamma^2}{32\omega^2} \left[8\omega^2 + (12\omega^2 - \gamma^2 + 8) e^{\gamma\pi/2\omega} + (4\omega^2 - \gamma^2 + 8) e^{\gamma\pi/\omega}\right] e^{-3\gamma\pi/2\omega}. \quad (23b)$$

We immediately see that the backscattering is greater if $\gamma_2 > \gamma_1$ ($\delta > 0$) than if γ_1 is the larger friction coefficient. This behavior is similar to that which occurs when we have kinetic friction. Thus, again a force in the second granule is more effective in producing the backscattering (as expected). In Fig. 7, we present the velocity of the first granule at the end of the collision as a function of γ for different values of δ . Once again we find (for each value of δ) an optimal scaled dissipation constant for which the backscattering is greatest. We note that the total energy at the end of the collision is a monotonically decreasing function of the average dissipation parameter γ .

IV. SUMMARY AND OUTLOOK

We have presented an overview of the dynamics of two granules subject to repulsive but not restoring forces (as in granular materials), and to kinetic or hydrodynamic friction. In particular, we explored parameter regimes that would give rise to backscattering *and* propagation at the end of a collision, with a view toward future studies of chains of granules subject to friction. We explored the consequences of “frictional disorder” in the two-granule system and found dramatically asymmetric behavior, that is, backscattering and propagation are affected differently by the friction on the first and second granules. For example, while friction that is “too high” on either granule will lead to situations where backscattering or propagation or both do not occur, the range of friction parameters that *do* lead to the occurrence of backscattering *and* propagation is considerably greater for the second granule than for the first. While this is perhaps not surprising, the nonmonotonocities in the final velocity and energy as a function of friction point to the interesting dynamical asymmetries in this problem. While most of our results have been calculated for a potential with $n = 2$ [cf. Eq. (1)], we have argued and shown numerically that the two-granule results are qualitatively

similar for other values of n (albeit not quantitatively equal). They therefore provide some insights into the dynamics involving more realistic potentials.

Finally, we stress that a chain of many granules differs in important ways from the two-granule system. For example, with $n > 2$ a frictionless chain may support solitons while the $n = 2$ chain does not [3]. Also, due to the interactions with further granules, there may be backscattering in a chain even for parameters that do not lead to backscattering in the two-granule system. On the other hand, since pulses are known to remain very narrow in granular chains [2, 5, 6], the analysis of the dynamics of two granules provides important insights into the behavior of longer chains and other larger arrays [18].

Acknowledgments

This work was supported by the Engineering Research Program of the Office of Basic Energy Sciences at the U. S. Department of Energy under Grant No. DE-FG03-86ER13606.

APPENDIX A: SCALING

The equations of motion with kinetic friction are in general of the form

$$m\ddot{y}_i(\tau) = \pm\mu_i g - a[y_i(\tau) - y_j(\tau)]^{n-1} \quad (\text{A1})$$

where the y 's are displacements, τ is the time, n is the exponent in Eq. (1), μ_i is the friction coefficient, g is the gravitational constant, and $i, j = 1, 2$. If particle i is frictionless, the first term on the right is absent. The initial conditions are $y_i(0) = 0$ and $\dot{y}_i(0) = 0$ or v_0 . We define new variables x_i and t via the relations,

$$y_i = Ax_i, \quad \tau = Bt, \quad (\text{A2})$$

in terms of which the equations of motion are

$$\frac{mA}{B^2}\ddot{x}_i(t) = \pm\eta_i - aA^{n-1}[x_i(t) - x_j(t)]^{n-1}. \quad (\text{A3})$$

The choices

$$A = \left(\frac{v_0^2 m}{a}\right)^{1/n}, \quad B = \frac{1}{v_0} \left(\frac{v_0^2 m}{a}\right)^{1/n}, \quad \eta \equiv \frac{\mu g}{mv_0^2} \left(\frac{v_0^2 m}{a}\right)^{1/n} \quad (\text{A4})$$

lead to the scaled equations of motion used in the text, e.g.

$$\ddot{x}_i(t) = \pm\eta_i - [x_i(t) - x_j(t)]^{n-1}, \quad (\text{A5})$$

with the initial conditions $x_i(0) = 0$ and $\dot{x}_i(0) = 0$ or 1.

With hydrodynamic friction the equations of motion are of the form

$$m\ddot{y}_i(\tau) = -\tilde{\gamma}_i \dot{y}_i(\tau) - a[y_i(\tau) - y_j(\tau)]^{n-1} \quad (\text{A6})$$

and, in terms of the new variables,

$$\frac{A}{B^2}\ddot{x}_i(t) = -\tilde{\gamma}_i \frac{A}{B}\dot{x}_i(t) - aA^{n-1}[x_i(t) - x_j(t)]^{n-1}. \quad (\text{A7})$$

Again we choose A and B as above, and set

$$\gamma_i = \frac{\tilde{\gamma}_i}{mv_0} \left(\frac{v_0^2 m}{a}\right)^{1/n} \quad (\text{A8})$$

to obtain

$$\ddot{x}_i(t) = -\gamma_i \dot{x}_i - [x_i(t) - x_j(t)]^{n-1} \quad (\text{A9})$$

with initial conditions as above.

[1] H. M. Jaeger S. R. Nagel, *Science* **255**, 1523 (1992).

- [2] *The Granular State*, edited by S. Sen and M. Hunt, MRS Symp. Proc. **627** (Pittsburgh, PA, 2001).
- [3] V. F. Nesterenko, *J. Appl. Mech. Tech. Phys.* **5**, 733 (1983).
- [4] R. S. Sinkovits and S. Sen, *Phys. Rev. Lett.* **74**, 2686 (1995).
- [5] T. R. Krishna Mohan and S. Sen, cond-mat/0304600.
- [6] S. Sen *et al.*, in *Modern Challenges in Statistical Mechanics: Patterns, Noise and the Interplay of Nonlinearity and Complexity*, edited by V. M. Kenkre and K. Lindenberg, AIP Conference Proceedings **658**, 357 (2003).
- [7] S. Sen, M. Manciu, and J. D. Wright, *Phys. Rev. E* **57**, 2386 (1998).
- [8] C. Coste, E. Falcon, and S. Fauve, *Phys. Rev. E* **56**, 6104 (1997).
- [9] A. Rogers and C. G. Don, *Acoust. Austral.* **22**, 5 (1994).
- [10] M. J. Naughton *et al.*, IEEE Conf. Proc. **458**, 249 (1998).
- [11] H. Hertz, *J. reine u. angew. Math.* **92**, 156 (1881).
- [12] L. D. Landau and E. M. Lifshitz, *Theory of Elasticity* (Addison- Wesley, Massachusetts, 1959), pp. 30.
- [13] For reviews see S. Flach and C. R. Willis, *Physics Reports* **295**, 181 (1998); *ibid*, *Physica D*, 119, 1 (1999); S. Aubry, *Physica D* **103**, 201 (1997).
- [14] R. Reigada, A. Sarmiento, and K. Lindenberg, to appear in *Chaos* (2003) and references therein.
- [15] Mackay, R. S., *Phys. Lett. A* **251**, 191 (1999).
- [16] Sen, S. and Manciu, M., *Phys. Rev. E* **64**, 056605 (2001).
- [17] M. Nakagawa, J. H. Agui, D. T. Wu, and D. V. Extramiana, *Granular Matter* **4**, 167 (2003).
- [18] A. Rosas, D. ben-Avraham, and K. Lindenberg, in progress.